JOURNAL OF CATALYSIS 99, 375–382 (1986)

Catalysis by Amorphous Metal Alloys

V. Hydrogenation of Carbon Monoxide over Amorphous $Ni_{78}P_{19}La_3$ Ribbon Alloy

HIROMI YAMASHITA, MASAHITO YOSHIKAWA, TAKUZO FUNABIKI,
AND SATOHIRO YOSHIDA

Department of Hydrocarbon Chemistry and Division of Molecular Engineering, Faculty of Engineering, Kyoto University, Kyoto 606, Japan

Received October 7, 1985; revised January 23, 1986

Amorphous Ni–P–La as well as Ni–P alloys exhibited high catalytic activity for hydrogenation of carbon monoxide to produce C_1 and C_2 hydrocarbons, when the alloys were pretreated with a dilute nitric acid solution, oxygen and hydrogen successively. The turnover frequency (TF) values were much higher than those over Ni/Al_2O_3, while the values over the crystallized alloys were comparable to those over Ni/Al_2O_3. The temperature in the oxygen treatment affected TF values significantly. Addition of a small amount of lanthanum to Ni–P amorphous alloy was effective for controlling the oxidation state of surface species, modifying the electronic state of the active sites, and brining about the enhancement of catalytic activity.

INTRODUCTION

Catalytic activities of amorphous metal alloys have attracted attention in recent years (*1–6*). In previous papers (*7–10*), we have reported on the hydrogenation of olefins over amorphous and crystallized Ni–P and Ni–B alloys, laying stress on the effects of pretreatment. The important points which have been clarified are: (1) the pretreatments with acid, oxygen, and hydrogen bring about not only the increase in the numbers of active sites but also the change of their electronic states; (2) the electron deficient nickel atoms generated by the oxidation of nickel and phosphorous are effective for the activation of molecular hydrogen; (3) the structural change which is not detected by XRD is important for the generation of electron-deficient nickel; (4) the amorphous alloy is highly active in comparison with the crystallized alloy because of the greater homogeneity of the former.

It is well known that nickel catalyzes hydrogenation of carbon monoxide. Komiyama and co-workers have already reported the characteristics of amorphous Ni–P alloys for the reaction (*1*). However, they neither noticed the effects of pretreatments nor investigated the surface states of the alloys. Additive lanthanum is reported to affect the catalytic activity of transition metals significantly (*11*), but there has been no published result about the catalysis by Ni–P–La amorphous alloys. In the present study, we carried out the catalytic hydrogenation of carbon monoxide over amorphous and crystallized Ni–P–La and Ni–P alloys, focusing our main attention on the effects of lanthanum on the catalytic activity as well as on the surface states of the alloys which are pretreated in the same manner described above.

EXPERIMENTAL

Catalysts and hydrogenation of carbon monoxide. Ni–P–La (P 19 atom%, La 3.2 atom%) and Ni–P (P 19 atom%) alloys in the form of ribbons of ca. 2 mm wide and 10–20 μm thick were prepared by the rapid quenching method using a single steel roll (*8*). The alloys were pretreated with a 6 mol dm^{-3} HNO_3 solution for 10 min at room temperature. After washing and drying, the alloys were treated with oxygen (16.7 kPa) for 1 h at a given temperature and finally

0021-9517/86 $3.00

with hydrogen (13.3 kPa) for 2 h at 573 K in a reaction vessel. The BET surface area was measured by a standard method using krypton physisorption at 77 K and found as 0.23 and 0.14 m^2g^{-1} for amorphous Ni–P–La and Ni–P alloys, respectively. Differential thermal analysis (DTA) by a Dupont 990 DSC apparatus indicated that the amorphous Ni–P alloy set in to crystallize at 643 K, while the amorphous Ni–P–La was more stable to heating and began to crystallize at 743 K. The hydrogenation of carbon monoxide was carried out in a conventional closed-circulation reaction system (300 cm^3) at 573 K. The reaction temperature was varied between 513 and 573 K for estimation of activation energies. A standard initial pressure was 22.0 kPa for hydrogen and 4.7 kPa for carbon monoxide. The initial rate which was estimated from the initial pressure change was used as a measure of activity. Products were analyzed by GLC using a 2-m column of Porapack Q.

Chemisorption of carbon monoxide and hydrogen. The chemisorption isotherms of carbon monoxide and hydrogen were measured at room temperature using a calibrated Pirani vacuum gauge (ULVAC GP-2T) as reported previously (*10*).

ESCA spectra. ESCA spectra were recorded with Shimadzu ESCA-750 using Mg radiation (8 kV and 30 mA) as described previously (*10*). The binding-energy values were referred to the value of the contaminant carbon (C_{1s} = 285.0 eV) for convenience.

RESULTS

Hydrogenation of Carbon Monoxide

Both Ni–P–La and Ni–P alloys as quenched exhibited little activity to the hydrogenation of carbon monoxide at 573 K, but, after the pretreatments described in experimental section, the reaction proceeded at a measurable rate. In the previous works about hydrogenation of olefins (*10*), the effect of oxygen pretreatment was found to be more profound than that of hydrogen pretreatment. Thus, in the present study, our attention was focused on the effect of the former. We compared the catalytic activity, chemisorption capacity and ESCA spectra of alloys pretreated with oxygen at different temperatures.

Figure 1 shows the change of catalytic activity by the temperature in the oxygen treatment. In the figure, the results over crystallized alloys are also included. The crystallization was accomplished by heating the Ni–P–La alloy at 773 K for 3 h and the Ni–P alloy at 723 K for 3 h under vacuum. In the cases of amorphous alloys, an enhancement in the activity was observed at temperatures above 473 K and the maximum activity was observed at 513 K. In the case of crystallized Ni–P–La alloy, the activity was much smaller than that of amorphous alloy and increased gradually with the treatment temperature over the range of temperatures studied. Products were methane and ethane, and hydrocarbons with more than three carbon atoms were not produced. Figure 2 shows the selectivity to ethane at the reaction time of 30 min. The

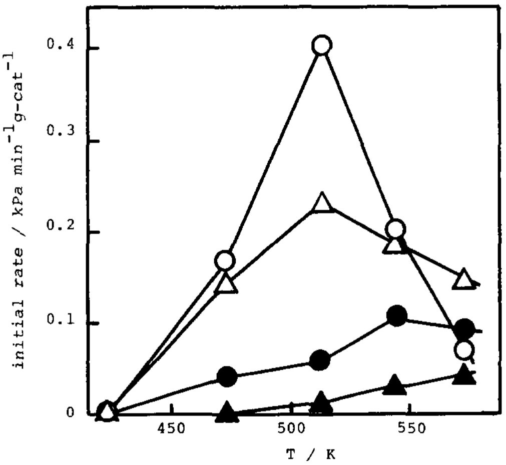

FIG. 1. Effect of oxygen pretreatment of the Ni–P–La and Ni–P alloys on the initial rate of hydrogenation of CO. Initial pressure P_{H_2} = 22.0 kPa and P_{CO} = 4.7 kPa; reaction temperature, 573 K. The alloys pretreated with a dilute HNO_3 solution, 6.7 kPa oxygen for 1 h and 13.3 kPa hydrogen at 573 K for 2 h. (△) Amorphous and (▲) crystallized Ni–P–La; (○) Amorphous and (●) crystallized Ni–P alloy.

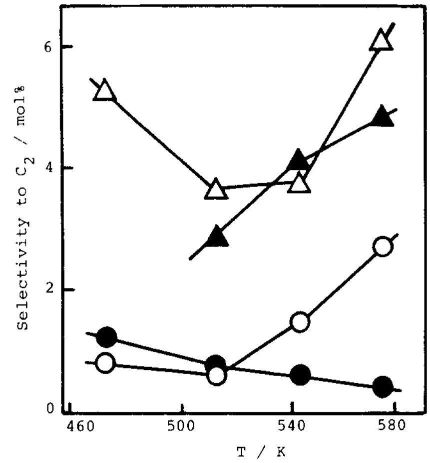

FIG. 2. Effect of the oxygen pretreatment on selectivity to ethane. (△) Amorphous and (▲) crystallized Ni–P–La alloy; (○) amorphous and (●) crystallized Ni–P alloy. Pretreatment and reaction conditions: see caption to Fig. 1.

addition of lanthanum was effective for increasing selectivity to ethane.

There was no evidence in XRD patterns for the crystallization of Ni–P–La and Ni–P amorphous alloys after 30 min of the reaction time. Especially, the Ni–P–La alloy was in an amorphous state even after 10 h, while the Ni–P exhibited weak peaks due to $Ni_{12}P_5$ and Ni metal in XRD patterns after 10 h.

A kinetic study over the amorphous alloys was carried out by varying the partial pressure of carbon monoxide or hydrogen at 573 K. The reaction orders were estimated from the logarithmic plots of normalized rate against ln P as shown in Fig. 3. The orders were 0.8 and −0.03 with respect to hydrogen and carbon monoxide, respectively, over the Ni–P–La alloy, and 1.0 and −0.7, respectively, over Ni–P alloy. Thus the rate equations are expressed as

$$r = k_1 P_{H_2}^{0.8} P_{CO}^{-0.03} \text{ for Ni–P–La,}$$

$$r = k_2 P_{H_2}^{1.0} P_{CO}^{-0.7} \text{ for Ni–P.}$$

The activation energies were estimated as 84.9 and 93.7 kJ mole^{-1} for the Ni–P–La and Ni–P alloys, respectively, from the initial rates over the temperature range of 513 to 573 K. These values were smaller than that (104.6 kJ mole^{-1}) over 5 wt% Ni/Al_2O_3 (*12*).

Chemisorptions of Carbon Monoxide and Hydrogen

Carbon monoxide and hydrogen uptakes were measured with the alloys pretreated as described above. The number of surface nickel atoms was estimated from the results of chemisorption by assuming an adsorption equilibrium according to Langmuir isotherm. The assumption of the single-site adsorption of carbon monoxide or dissociative adsorption of hydrogen was supported by good linear Langmuir plots and the absence of substantial dependence of the values on the kind of adsorbate. Figure 4 shows the effect of temperature of the oxygen treatment on the number of surface nickel atoms which is the mean value of the

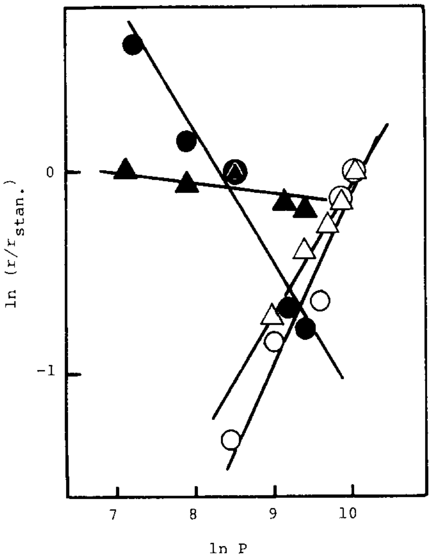

FIG. 3. Dependence of the initial rates of hydrogenation of CO on the partial pressures of H_2 and CO. Dependence of P_{CO} at P_{H_2} = 22.0 kPa; (▲) amorphous Ni–P–La and (●) amorphous Ni–P alloy. Dependence on P_{H_2} at P_{CO} = 4.7 kPa; (△) amorphous Ni–P–La and (○) amorphous Ni–P alloy. The alloys were pretreated with a dilute HNO_3 solution, 6.7 kPa oxygen at 513 K for 1 h and 13.3 kPa hydrogen at 573 K for 2 h. Reaction temperature, 573 K. The initial rates (r) were normalized to those ($r_{stan.}$) under P_{H_2} = 22.0 kPa and P_{CO} = 4.7 kPa.

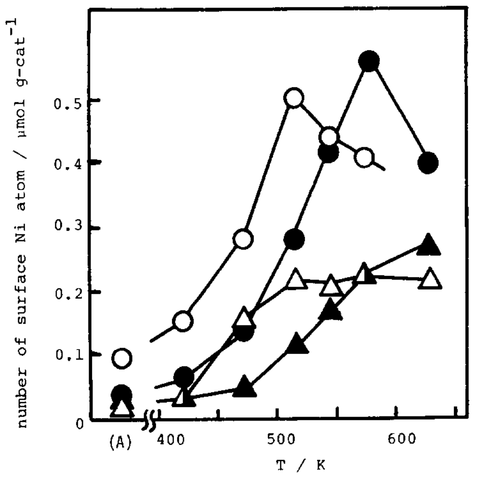

FIG. 4. Effect of the temperature of the oxygen pretreatment on the number of surface nickel atoms. (△) Amorphous and (▲) crystallized Ni–P–La alloy; (○) amorphous and (●) crystallized Ni–P alloy. The values at (A) correspond to those measured without pretreatment. Pretreatment conditions: see caption to Fig. 1.

results from carbon monoxide and hydrogen uptakes. The number for amorphous Ni–P–La alloy increased gradually with the temperature above 473 K and attained constant values at above 513 K. These values were small and the change was somewhat moderate compared with those of the Ni–P amorphous alloy. The change in the number for crystallized alloys was much smaller than that for amorphous alloys and a higher temperature of oxygen treatment was necessary to obtain the same value as that for the amorphous alloys.

By using the number of surface nickel atoms estimated by the way mentioned above, the turnover frequency (TF) was calculated for the hydrogenation of carbon monoxide under a given condition (573 K, P_{CO} = 4.6 kPa, P_{H_2} = 21.9 kPa) (Table 1). The TF values over amorphous Ni–P–La alloys were high and the change of TF value with the temperature of the treatment with oxygen was moderate, compared with those over amorphous Ni–P alloys. The TF values for the amorphous alloys were much greater than those for the crystallized alloys and 5 wt% Ni/Al_2O_3 (*12*).

ESCA Spectra

A set of ESCA spectra are shown in Fig. 5 for the amorphous Ni–P–La and Ni–P alloys after pretreatments. The spectra of Ni–P–La alloy, which was treated with oxygen at 513 K, are comprised of two peaks of nickel ($2p_{3/2}$; 856.5, 853.4 eV), two peaks of phosphorus ($2p$; 133.8, 129.7 eV), and three peaks of lanthanum ($3d_{5/2}$; 840.2, 838.7, 835.9 eV). The Ni($2p_{3/2}$) peak at 853.4 eV and P($2p$) peak at 129.7 eV are assignable to metallic nickel and elemental phosphorus. The values corresponding to pure nickel metal and red phosphorus are reported as 852.2 eV (*13*) and 130.4 eV (*14*), respectively. Thus, for amorphous Ni–P–La alloys, the metallic nickel atoms are in an electron-deficient state, while the elemental phosphorus atoms are in an electron-rich state. Similar results were also obtained for the Ni–P amorphous alloys. Other peaks of Ni($2p_{3/2}$) (856.5 eV) and P($2p$) (133.8 eV) are assignable to nickel oxide and phosphorus oxide. Among three peaks of La($3d_{5/2}$), the peak at 835.9 eV is assignable to metallic lanthanum and the peaks at 840.2 and 838.7 eV might correspond to La_2O_3 and $La(OH)_3$, respectively.

TABLE 1

Turnover Frequencies for CO Hydrogenation over Amorphous and Crystallized Ni–P–La and Ni–P Alloys Pretreated with Oxygen at Various Temperatures

Oxidation temp. (K)	Turnover frequency (s^{-1})			
	Ni–P–La		Ni–P	
	Amor.	Cryst.	Amor.	Cryst.
473	0.86	0.0	0.48	0.24
513	0.88	0.06	0.67	0.17
543	0.79	0.11	0.38	0.20
573	0.52	0.16	0.14	0.08
5% Ni/Al_2O_3	0.05[a]			

Note. Initial pressure, P_{H_2} = 22.0 kPa and P_{CO} = 4.7 kPa; reaction temperature, 573 K. Pretreatment conditions: see caption to Fig. 1.

[a] Vannice, Ref. (*12*).

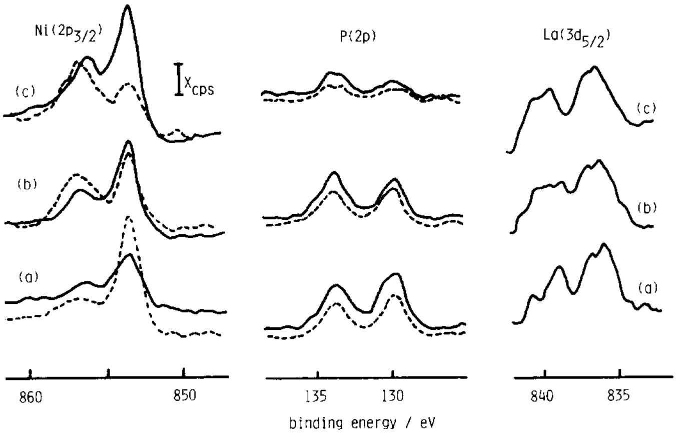

FIG. 5. ESCA spectra of the amorphous (—) Ni–P–La and (---) Ni–P alloys pretreated with oxygen at different temperatures for 1 h; (a) 423, (b) 513, and (c) 573 K. Spectra were recorded after reduction with hydrogen at 573 K for 2 h. Scale of peak intensity (X_{cps}) for Ni($2p_{3/2}$): Ni–P–La (a)–(c) 1000, Ni–P (a), (b) 1000 and (c) 500; for P($2p$): Ni–P–La and Ni–P (a)–(c) 500; for La($3d_{5/2}$): Ni–P–La (a)–(c) 200.

The binding energy of pure lanthanum metal is reported as 832.0 eV (*15*) and Siegmann and co-workers reported that the binding energies of La in La_2O_3 and $La(OH)_3$ are higher than that of metallic lanthanum by 4.5 and 3.7 eV, respectively (*16*).

The binding energies of Ni($2p_{3/2}$) and P($2p$) mentioned above changed little by the oxygen treatments, but the intensities of the peaks changed significantly. The intensities of the two Ni($2p_{3/2}$) peaks increased with increasing the temperature of the pretreatments with oxygen. The two sharp P($2p$) peaks disappeared on the alloy pretreated at 573 K. The ESCA spectra of Ni–P amorphous alloy were also shown in Fig. 5 for comparison. The oxidation of nickel was suppressed in the Ni–P–La alloy, compared with that in the Ni–P alloy. The oxidation states of surface phosphorus species were very similar on both alloys. The absolute intensities of La($3d_{5/2}$) peaks were small and so their change with the temperature of oxygen pretreatment can not be discussed clearly. However, the intensity of La($3d_{5/2}$) peak at 840.2 eV increased distinctly with the temperature of oxygen pretreatment. This result suggested that lanthanum segregated out mainly as La_2O_3 by the oxygen pretreatment.

Figure 6 shows the ESCA spectra of amorphous and crystallized Ni–P alloys, which were treated with oxygen at 517 K and followed by reduction with hydrogen. In comparison with amorphous alloy, oxidation of the crystallized alloy proceeded more deeply inside the bulk of alloy and also the ratios of the peak intensities of oxidized against nonoxidized species of nickel, phosphorus, and lanthanum were high.

DISCUSSION

Effects of Lanthanum on the Stability of Amorphous Structure

As shown in Fig. 1, the rates of hydrogenation of carbon monoxide over Ni–P–La and Ni–P alloys depend on the temperature of the oxygen treatment. As reported previously (*10*), the oxygen treatment of Ni–P amorphous alloy brings about the increase in the numbers of surface active sites and the change of their electronic state. The results of chemisorption (Fig. 4) and ESCA spectra (Fig. 5) indicate that the number of the surface nickel atoms and the total concentration of nickel species in the surface layers (slightly inside the bulk) increase with the temperature of the oxygen treatment, but the change in the number of the

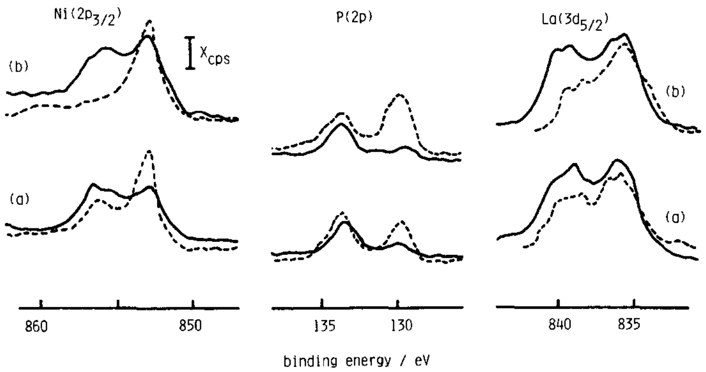

FIG. 6. ESCA spectra of the (—) crystallized alloy in comparison with (---) amorphous alloy. Pretreatment: O_2, 513 K, 1 h; H_2, 573 K, 2 h. Sputtering by Ar^+: (a) none and (b) 20 mA, 5 min (approximate depth, 25 nm). Scale of peak intensity (X_{cps}) for Ni($2p_{3/2}$): (a), (b) 1000; for P($2p$): (a), (b) 500; for La($3d_{5/2}$): (a), (b) 200.

surface nickel atoms of Ni–P–La amorphous alloy was less significant in comparison with Ni–P alloy. We have proposed that the increase in the number of the surface nickel atoms is due to the formation of nickel oxide in the surface layers which facilitates the diffusion of electron-deficient nickel atoms formed in the bulk to the surface layers and the diminution of phosphorus species in the surface (*10*). The oxidation of nickel species in the surface layers is essential for the increase in the number of the surface nickel atoms. In the case of amorphous Ni–P–La alloy, the increase in the number of the surface nickel atoms was somewhat moderate and the intensities of ESCA peak of nickel oxide relative to metallic nickel was small in comparison with amorphous Ni–P alloy. Thus, the additive lanthanum is effective to depress the change of the structure accompanied by the increase in the number of surface nickel atoms.

The amorphous structure of Ni–P–La alloy is more stable than that of Ni–P alloy as revealed by differential thermal analysis and XRD. The following may be probable reasons for the stabilization of amorphous structure by the addition of a small amount of lanthanum. (1) As shown in ESCA spectra in Fig. 5 which indicate the presence of the lanthanum oxide and the electron-deficient metallic lanthanum in the Ni–P–La amorphous alloy, electrons may be transferred from lanthanum to nickel or phosphorus and from nickel or phosphorus to lanthanum oxide. The interaction between lanthanum and nickel or phosphorus species may be effective to stabilize the amorphous structure. (2) The large atomic radius of lanthanum in comparison with those of nickel and phosphorus is less favorable for the migration of atoms which brings about the structural reconstruction toward the metastable state.

Effect of Lanthanum on the Surface State

The change in the electronic state of the surface nickel is important for the generation of high catalytic activity and an effect in the activity by the addition of lanthanum is reflected on the TF value. As shown in Table 1, the TF values for the amorphous alloys were about one order of magnitude greater than that for 5 wt% Ni/Al_2O_3. The high TF values over amorphous alloys indicate the formation of the highly active surface nickel atoms in the optimum electronic state by the pretreatment.

In a previous study on the hydrogenation of olefins over Ni–P amorphous alloy (*10*), we have proposed that the formation of electron-deficient nickel atoms is essential for the high TF values and that the electron-deficient nickel atoms are effective for the activation of hydrogen molecule, based on a kinetic study (*8*). These electron-deficient nickel atoms are formed when a part of surface nickel and phosphorus species are oxidized to stable oxides by the treatment with oxygen and the electron transfer from nickel atoms to these oxides, especially to nickel oxide. In the hydrogenation of CO over Ni–P–La and Ni–P amorphous alloys, the treatment with oxygen at temperatures above 473 K was necessary to generate the high catalytic activity, indicating that the formation of electron-deficient nickel atoms is also essential for the reaction. The TF value of Ni–P amorphous alloy for the hydrogenation of olefins increased monotonously with increase of temperature of the oxygen treatment in the range of 473–573 K (*10*). Based on the ESCA and TPR results, this monotonous increase in TF value of Ni–P amorphous alloy was related to the increase in the strength of the Ni—O bonds of nickel oxides and in the amount of nickel oxides in the surface layers which promote the electron transfer from nickel to nickel oxides increasing the electron deficiency of nickel atoms. On the other hand, the TF value of Ni–P amorphous alloy for the hydrogenation of CO became maximum at 513 K and decreased by the treatment at higher temperatures. This result is supposed to indicate that the temperate deficiency in the electron density on nickel atoms are necessary for the high catalytic activity for the hydrogenation of CO.

As shown in Table 1, the TF values are greater and the change in TF values with the temperature of the oxygen treatment is smaller over Ni–P–La amorphous alloy than those over Ni–P amorphous alloy. This seems to be related to the different stability of amorphous structure between Ni–P–La and Ni–P alloys. In the case of Ni–P amorphous alloy, the oxidation of surface nickel may bring about the reconstruction of surface layers (slightly inside the bulk) accompanied by the generation of discontinuity of surface structure which cannot be detected by XRD. This reconstruction of surface layers will promote the oxidation of nickel species in the surface layers, strengthening the Ni—O bonds of nickel oxides and increasing the electron deficiency of nickel atoms. In the case of Ni–P–La amorphous alloy, the reconstruction of surface layers caused by the oxidation of surface nickel is suppressed in comparison with Ni–P amorphous alloy. This will result in the suppression of excessive oxidation of nickel species in the surface layers and the formation of the nickel atoms with a favorable state on the surface.

The TF values shown in Table 1 indicate that the crystallization brings about the great drop of activity. ESCA spectra shown in Fig. 6 indicate that the oxidation of nickel, phosphorus, and lanthanum proceeds more deeply inside the bulk of crystallized alloy in comparison with amorphous alloy. Discontinuity and the aggregation of nickel in the surface proceed greatly enough to be detected by XRD. The similar aggregation of nickel species accompanying the crystallization occurs over Ni–B alloy and affects the catalytic activity for the hydrogenolysis of alkane (structure-sensitive reaction) (*9*). The profound aggregation of nickel species is accompanied by the separation of nickel from other species. This weakens the interaction between nickel and other species, inhibiting the formation of the electron-deficient nickel atoms on the surface. The similar decrease in the interaction between nickel and other species due to the crystallization of amorphous alloys has been observed with Ni–Fe–P–B and Ni–B alloys as shown by the smaller shifts of the peaks of nickel in ESCA spectra of crystallized alloys than those of amorphous alloys (*9*, *17*).

The reaction rates obeyed negative and almost zeroth-order kinetics to the partial pressure of CO over Ni–P alloy and over Ni–P–La alloy, respectively (Fig. 3). The mechanism of the reaction with three steps has been proposed for the hydrogenation of CO to methane (*18–20*): (1) the adsorption of CO and H_2; (2) the cleavage of C—O bond to produce CH_x species; (3) the hydrogenation of CH_x species with activated hydrogen atom. As reported previously (*8*, *10*), the activation of molecular hydrogen proceeds easily on the electron-deficient nickel species. The negative-order kinetics to the partial pressure of CO over Ni–P alloy indicates that the formation of CH_x species accompanied by the cleavage of C—O bond is suppressed by the adsorbed CO covered on the active surface sites. As discussed above, highly electron-deficient nickel atoms would exist on Ni–P amorphous alloy. The limited electron back-donation from highly electron-deficient nickel atoms to an antibonding orbital of an adsorbed CO molecule suppresses the cleavage of C—O bond (*21*). In the case of Ni–P–La alloys, the reaction rates were independent of partial pressure of CO, indicating that adsorption of CO is strong enough but not to strong to retard the reaction. As discussed above, the nickel atoms would be in a moderately electron-deficient state, which is effective to electron back-donation to an antibonding of an adsorbed CO molecule leading to the cleavage of the C—O bond.

In conclusion, the electronic state of the surface-active nickel species is dependent on the amount of nickel oxide in the surface layers (slightly inside the bulk). The moderate oxidation of surface species and the thermal stability of the surface structure are necessary to bring about the stable high catalytic activity for the hydrogenation of carbon monoxide over amorphous alloy. The addition of the small amount of third component, such as lanthanum, to the bimetallic amorphous alloy is effective in controlling the oxidation of surface species and in modifying the electronic states of surface active sites.

REFERENCES

1. Yokoyama, A., Komiyama, H., Inoue, H., Masumoto, T., and Kimura, H. M., *J. Catal.* **68,** 355 (1981); *J. Non-Cryst. Solids* **61** and **62,** 619 (1984).
2. Carturan, G., Cocco, G., Baratter, E., Navazio, G., and Antonione, C., *J. Catal.* **90,** 178 (1984).
3. Smith, G. V., Zahraa, O., Molnar, A., Khan, M. M., Rihter, B., and Brower, W. E., *J. Catal.* **83,** 238 (1983).
4. Imanaka, T., Tamaki, J., and Teranishi, S., *J. Chem. Soc. Japan,* 1064 (1985).
5. Yamashita, H., Yoshikawa, M., Kaminade, T., Funabiki, T., and Yoshida, S., *J. Chem. Soc., Faraday Trans. 1,* in press. (Part 3 of this series.)
6. Yamashita, H., Kaminade, T., Funabiki, T., and Yoshida, S., *J. Mater. Sci. Lett.* **4,** 1241 (1985).
7. Yoshida, S., Yamashita, H., Funabiki, T., and Yonezawa, T., *J. Chem. Soc., Chem. Commun.,* 964 (1982).
8. Yoshida, S., Yamashita, H., Funabiki, T., and Yonezawa, T., *J. Chem. Soc., Faraday Trans. 1* **80,** 1435 (1984). (Part 1 of this series.)
9. Yamashita, H., Funabiki, T., and Yoshida, S., *J. Chem. Soc., Chem. Commun.,* 868 (1984).
10. Yamashita, H., Yoshikawa, M., Funabiki, T., and Yoshida, S., *J. Chem. Soc., Faraday Trans. 1* **81,** 2485 (1985). (Part 2 of this series.)
11. Somorjai, G. A., and Davis, S. M., *CHEMTECH,* August, 502 (1983).
12. Vannice, M. A., *J. Catal.* **37,** 462 (1975).
13. Nemoshkalenko, V. V., Kharlamov, A. I., Serebryakova, T. I., and Aleshin, V. G., *Kinet. Katal.* **19,** 1567 (1978).
14. Okamoto, Y., Nitta, Y., Imanaka, T., and Teranishi, S., *J. Chem. Soc., Faraday. Trans. 1* **75,** 2027 (1979).
15. Wagner, C. D., Riggs, W. M., Davis, L. E., Moulder, J. F., and Muilenberg, G. E., *in* "Handbook of X-Ray Photoelectron Spectroscopy." Perkin–Elmer Co., Physical Electronics Division, Eden Prarie, MN, 1979.
16. Siegmann, H. C., Schlapbach, L., and Brundle, C. R., *Phys. Rev. Lett.* **40,** 972 (1978).
17. Asami, K., Kimura, H. M., Hashimoto, K., Masumoto, T., Yokoyama, A., Komiyama, H., and Inoue, H., *J. Non-Cryst. Solids* **64,** 149 (1984).
18. Araki, M., and Ponec, V., *J. Catal.* **44,** 437 (1976).
19. Wentrcek, P. R., Wood, B. J., and Wise, H., *J. Catal.* **43,** 363 (1976).
20. Joyner, R. W., and Roberts, M. W., *J. Catal.* **50,** 176 (1977).
21. Bell, A. T., *Catal. Rev.-Sci. Eng.* **23,** 203 (1981).